

BABAR Results on $B \rightarrow X_s \gamma$

Jack L. Ritchie
 Department of Physics
 University of Texas at Austin
 Austin, TX 78712, USA
 Representing the BABAR Collaboration

Proceedings of CKM 2012, the 7th International Workshop on the CKM Unitarity Triangle, University of Cincinnati, USA, 28 September - 2 October 2012

1 Introduction

The flavor-changing neutral current process $b \rightarrow s \gamma$, shown in Figure 1, is of interest because it is one of the most reliably calculable of such processes in the Standard Model (SM) and also because many new physics scenarios (e.g., SUSY) may lead to deviations from the SM decay rate. Heavy-quark hadron duality implies this

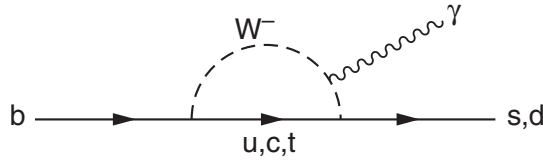


Figure 1: The electromagnetic penguin diagram responsible for $B \rightarrow X_s \gamma$ decays in the SM.

decay rate is very close to the decay rate for $B \rightarrow X_s \gamma$, where X_s represents any hadronic system containing a strange particle. The current next-to-next-to leading order calculation [1] gives:

$$\mathcal{B}(B \rightarrow X_s \gamma) = (3.15 \pm 0.23) \times 10^{-4},$$

for $E_\gamma > 1.6 \text{ GeV}$ (E_γ is the photon energy in the rest frame of the B meson). Measurements of the photon spectrum can constrain Heavy Quark Effective Theory parameters and help to reduce the uncertainties in the extraction of CKM elements $|V_{cb}|$ and $|V_{ub}|$ from semileptonic B decays.

Experimentally, measuring $\mathcal{B}(B \rightarrow X_s \gamma)$ is challenging. Multiple approaches are undertaken, each with strengths and weaknesses. BABAR's final results are presented

here for two of the alternative approaches. In one, a fully inclusive measurement is performed by detecting only the high-energy photon from the signal B decay, and using a lepton (e or μ) from the semileptonic decay of the other B in the event to suppress backgrounds. This method has the advantage of being inclusive, but the photon energy is smeared by the energy resolution of the electromagnetic calorimeter and also by the motion of the signal B in the $\Upsilon(4S)$ center of mass frame. A subtraction of backgrounds from other B decays ultimately leads to a systematic error that is larger than the statistical uncertainty. Also, this method does not distinguish $B \rightarrow X_s \gamma$ events from $B \rightarrow X_d \gamma$, so effectively they are combined. The second approach is a semi-inclusive measurement, in which a large number of exclusive modes are fully reconstructed and combined. This method has the virtue that the signal B is reconstructed, providing a precise determination of the photon energy in the B rest frame via the relation $E_\gamma = (m_B^2 - m_X^2)/(2m_B)$, but suffers from the fact that the measurement is not inclusive. Many modes are not included, and the uncertainty in estimating the missing modes introduces a systematic error that dominates the measurement. In both cases, all analysis procedures and event selection criteria were determined before they were applied to real data in the signal regions.

2 Fully Inclusive Results

The fully inclusive analysis [2, 3] used 347 fb^{-1} of data collected at the $\Upsilon(4S)$ at the SLAC PEP-II B-factory. The challenge is illustrated in Figure 2(a), which shows the expected SM signal, the B decay background, and the continuum background after

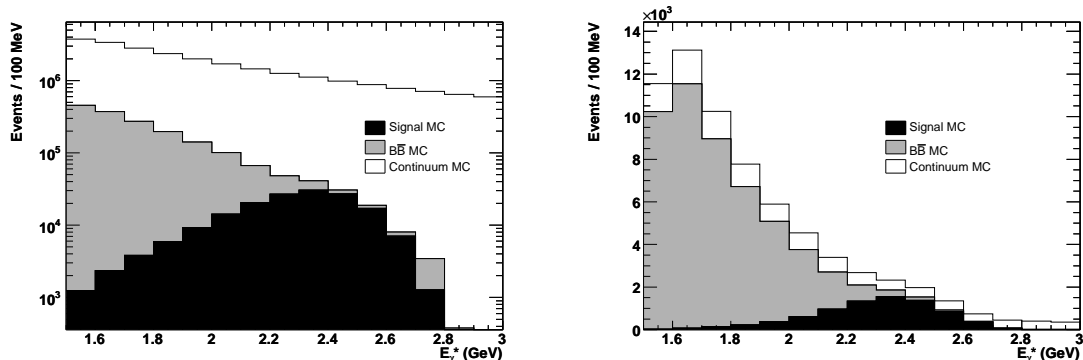


Figure 2: Monte Carlo signal and background yields versus E_γ^* : (a) after selecting a high-energy photon (log scale) and (b) after all selection criteria (linear scale).

selection of a high-energy photon satisfying $1.53 < E_\gamma^* < 3.5 \text{ GeV}$, where E_γ^* is the photon energy in the $\Upsilon(4S)$ rest frame. Figure 2(b) shows the situation after all event

selection criteria have been applied (achieving background rejection of about 10^{-5} with a signal efficiency of 2.6%). The large $B\bar{B}$ background can only be suppressed by imposing a cut on the photon energy, chosen to be $E_\gamma^* > 1.8$ GeV.

The remaining backgrounds are subtracted using Monte Carlo that is corrected using data control samples. The result for data, after $B\bar{B}$ background subtraction, is shown in Figure 3(a).

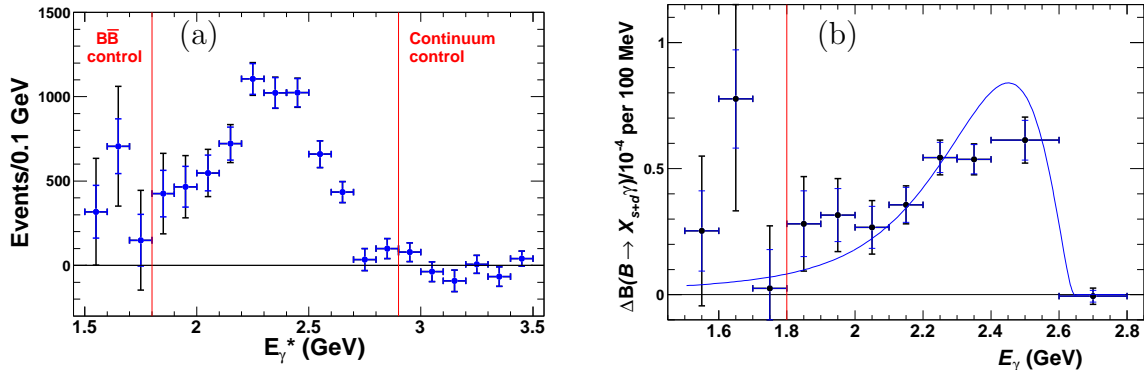


Figure 3: (a) Photon spectrum after background subtraction. The vertical lines indicate the boundaries of the blind signal region. Inner error bars indicate statistical errors only. (b) Photon spectrum after unfolding. The curve shows the spectrum in the kinetic scheme model using HFAG world average parameters normalized to data in the range $1.8 < E_\gamma^* < 2.8$ GeV.

The branching fraction is extracted from the event yield in the signal region defined by $1.8 < E_\gamma^* < 2.8$ GeV by applying a signal efficiency correction, corrections for smearing due to calorimeter energy resolution and motion of the signal B in the $\Upsilon(4S)$ frame, and a correction to account for $B \rightarrow X_d\gamma$ contamination (assuming the rates are related by CKM factors and using $1/(1 + |V_{td}/V_{ts}|^2) = 0.958 \pm 0.003$). The result is

$$\mathcal{B}(B \rightarrow X_s\gamma) = (3.21 \pm 0.15 \pm 0.29 \pm 0.08) \times 10^{-4},$$

for $E_\gamma > 1.8$ GeV, where the first error is statistical, the second is systematic, and the third represents the uncertainty in the signal efficiency from uncertainties in the model for the photon spectrum.

An unfolding procedure is applied to extract the photon spectrum in the B meson rest frame. This procedure corrects for calorimeter resolution smearing, smearing due to the motion of the B in the $\Upsilon(4S)$ rest frame, and corrects for detector and selection efficiencies. The unfolded spectrum is shown in Figure 3(b). In addition,

the first, second, and third moments of this spectrum, useful for determining Heavy Quark Effective Theory (HQET) model parameters, are reported in Reference [3].

A test for direct CP violation can be made by comparing the decay rates for B versus \bar{B} , using the charge of the tag lepton to separate the two categories. This measurement, which includes $B \rightarrow X_d \gamma$ events, is a strong test for new physics since the SM expectation[5] is negligibly different from zero. The result, in the optimized energy range $2.1 < E_\gamma^* < 2.8$ GeV, is

$$A_{CP} = \frac{\Gamma(B \rightarrow X_{s+d}\gamma) - \Gamma(\bar{B} \rightarrow X_{s+d}\gamma)}{\Gamma(B \rightarrow X_{s+d}\gamma) + \Gamma(\bar{B} \rightarrow X_{s+d}\gamma)} = 0.057 \pm 0.060 \pm 0.018.$$

3 Semi-inclusive Results

The semi-inclusive analysis [4] used 429 fb^{-1} of data and reconstructs the 38 exclusive modes listed in Table 1. Signal selection and background rejection is accomplished

$K_s \pi^+$	$K_s \pi^+ \pi^- \pi^+$	$K^+ \pi^+ \pi^- \pi^- \pi^0$	$K_s \eta \pi^+ \pi^-$
$K^+ \pi^0$	$K^+ \pi^+ \pi^- \pi^0$	$K_s \pi^+ \pi^- \pi^0 \pi^0$	$K^+ \eta \pi^- \pi^0$
$K^+ \pi^-$	$K_s \pi^+ \pi^0 \pi^0$	$K^+ \eta$	$K^+ K^- K^+$
$K_s \pi^0$	$K^+ \pi^+ \pi^- \pi^-$	$K_s \eta$	$K^+ K^- K_s$
$K^+ \pi^+ \pi^-$	$K_s \pi^0 \pi^+ \pi^-$	$K_s \eta \pi^+$	$K^+ K^- K_s \pi^+$
$K_s \pi^+ \pi^0$	$K^+ \pi^- \pi^0 \pi^0$	$K^+ \eta \pi^0$	$K^+ K^- K^+ \pi^0$
$K^+ \pi^0 \pi^0$	$K^+ \pi^+ \pi^- \pi^+ \pi^-$	$K^+ \eta \pi^-$	$K^+ K^- K^+ \pi^-$
$K_s \pi^+ \pi^-$	$K_s \pi^+ \pi^- \pi^+ \pi^0$	$K_s \eta \pi^0$	$K^+ K^- K_s \pi^0$
$K^+ \pi^- \pi^0$	$K^+ \pi^+ \pi^- \pi^0 \pi^0$	$K^+ \eta \pi^+ \pi^-$	
$K_s \pi^0 \pi^0$	$K_s \pi^+ \pi^- \pi^+ \pi^-$	$K_s \eta \pi^+ \pi^0$	

Table 1: 38 final states reconstructed, with $K_s \rightarrow \pi^+ \pi^-$, $\pi^0 \rightarrow \gamma \gamma$, and $\eta \rightarrow \gamma \gamma$.

using random forest classifiers trained on Monte Carlo signal and background samples. After reconstruction, events are binned as a function of the mass of the hadronic system, m_X , and maximum likelihood fits are performed in each of 18 mass bins to extract signal yields. Figure 4(a) shows the resulting m_X spectrum. The corresponding photon spectrum, shown in Figure 4(b), is obtained using $E_\gamma = (m_B^2 - m_X^2)/(2m_B)$.

The branching fraction is obtained summing the partial (bin-by-bin) branching fractions shown in Figure 4, giving the result:

$$\mathcal{B}(B \rightarrow X_s \gamma) = (3.29 \pm 0.19 \pm 0.48) \times 10^{-4},$$

for $E_\gamma > 1.9$ GeV. The first error is statistical and the second error is systematic. The systematic error, which dominates, is mainly due to the missing modes.

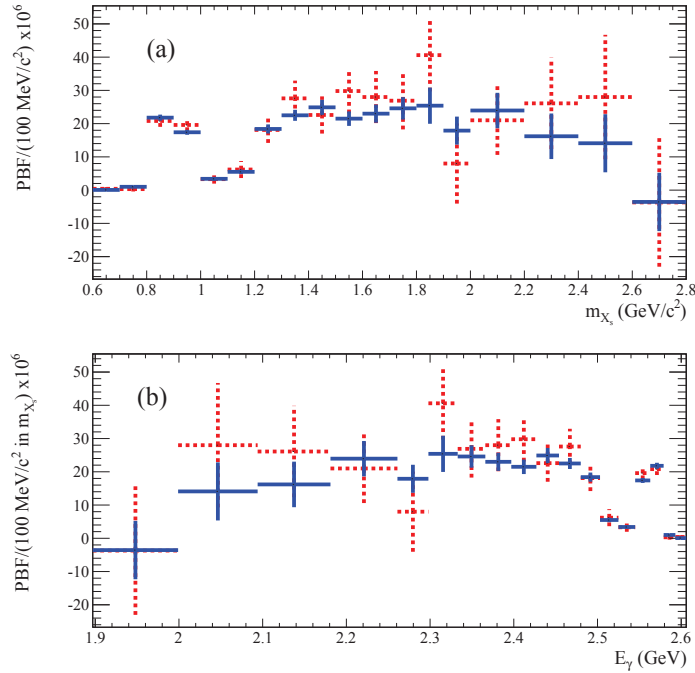


Figure 4: (a) Reconstructed hadronic mass spectrum and (b) the associated photon spectrum. The solid (blue) data points correspond to this measurement. The dashed (red) points are from an earlier *BABAR* measurement with 82 fb^{-1} .

Moments of the spectrum are also measured and the spectrum is fit to determine the parameters of HQET models. In particular, fits are performed to determine the parameters m_b and μ_b^2 in both the “kinetic” scheme and the “shape function” scheme. The results are given in Table 2.

	Kinetic scheme	Shape function scheme
m_b	$4.568^{+0.038}_{-0.036} \text{ GeV}/c^2$	$4.579^{+0.032}_{-0.029} \text{ GeV}/c^2$
μ_b^2	$0.450 \pm 0.054 \text{ GeV}^2$	$0.257^{+0.034}_{-0.039} \text{ GeV}^2$

Table 2: Results for HQET parameters based on fits to the m_X spectrum.

4 Conclusions

BABAR has reported final results from two analyses of $B \rightarrow X_s \gamma$, providing branching fractions, spectra, and spectral moments, as well as testing for direct CP violation.

The branching fraction measurements are in good agreement with the SM theory expectation, as shown in Figure 5. The figure shows comparable results of all experiments, extrapolated to a common energy cutoff of 1.6 GeV using the Heavy Flavor Averaging Group (HFAG) extrapolation factors [6].

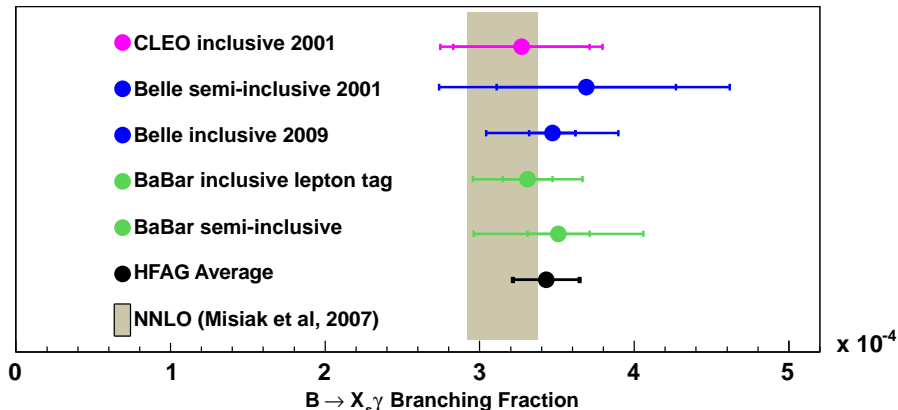


Figure 5: Summary of $B \rightarrow X_s \gamma$ branching fraction measurements: CLEO inclusive[7], Belle semi-inclusive[8], Belle inclusive[9], and the *BABAR* results presented here for inclusive[2, 3] and semi-inclusive[4]. The shaded region shows the SM theory expectation[1]. The current HFAG average[6] is also shown.

This work was supported in part by Department of Energy contract DE-AC02-76SF00515.

References

- [1] M. Misiak *et al.*, Phys. Rev. Lett. **98**, 022002 (2007).
- [2] J. P. Lees *et al.* [*BABAR* collaboration], Phys. Rev. Lett. **109**, 211801 (2012).
- [3] J. P. Lees *et al.* [*BABAR* collaboration], arXiv:1207.5772 [hep-ex]; to be published in Phys. Rev. D.
- [4] J. P. Lees *et al.* [*BABAR* collaboration], Phys. Rev. D **86**, 052012 (2012).
- [5] M. Benzke, S.J. Lee, M. Neubert, G. Paz, Phys. Rev. Lett. **106**, 141801 (2011).
- [6] <http://www.slac.stanford.edu/xorg/hfag/rare/2012/radll/btosg.pdf>
- [7] S. Chen *et al.*, [CLEO collaboration], Phys. Rev. Lett. **87**, 251807, (2001).

- [8] K. Abe *et al.*, [Belle collaboration], Phys. Lett. B **511**, 151158 (2001).
- [9] A. Limosani *et al.*, [Belle collaboration], Phys. Rev. Lett. **103**, 241801 (2009).